Terra Nova

doi: 10.1111/ter.12119

The last major earthquakes along the Magallanes–Fagnano fault system recorded by disturbed trees (Tierra del Fuego, South America)

Antonio Pedrera,[1] Jesús Galindo-Zaldívar,[1,2] Ana Ruiz-Constán,[3] Fernando Bohoyo,[3] Pablo Torres-Carbonell,[4] Patricia Ruano,[1,2] Adolfo Maestro[3] and Lourdes González-Castillo[2]

[1]*Instituto Andaluz Ciencias de la Tierra, CSIC/Universidad de Granada, Granada 18002, Spain;* [2]*Departamento de Geodinámica, Universidad de Granada, Granada 18071, Spain;* [3]*Instituto Geológico y Minero de España, Madrid ES-28003, Spain;* [4]*Centro Austral de Investigaciones Científicas, CADIC-CONICET B, Ushuaia Tierra del Fuego, 9410, Argentina*

ABSTRACT

Forests situated above active fault zones may record hillslope evolution, thus holding information about recent seismic events. Lenga trees (*Nothofagus pumilio*) extend across the Magallanes–Fagnano fault system (MFFS), the active transform boundary between the South American and Scotia plates. Coseismic surface ruptures along the fault scarp tilt trees located uphill. During the interseismic period, tree growth curves the trunks. Annual tree rings from the study area show abrupt changes from concentric to asymmetric, allowing the timing of major historical earthquakes to be established. In this case, tree-ring analysis suggests rupture on the MFFS fault scarp in 1883 ± 5 and 1941 ± 10, coinciding with the February 1, 1879 (Modified Mercalli Scale, VI) and the December 17, 1949 (Ms 7.8) earthquakes in Tierra del Fuego. Our results provide evidence that this fault system was the source of these earthquakes, which has implications for seismic hazard in the study region.

Terra Nova, 0, 1–6, 2014

Introduction

A foremost challenge in seismic hazard studies is determining the source of major earthquakes that pre-date instrumental records. Palaeoseismology provides details on the timing, location and size of prehistoric (McCalpin, 2009) and historical earthquakes (Yeats and Prentice, 1996). Large earthquakes are capable of creating or modifying the topographic surface (e.g. Keller and Pinter, 2001). Surface rupture on active faults usually forms scarps and initiates erosive processes at the new topographic step. Although this process is more intense in normal and reverse faults, strike-slip faults can leave topographic signatures in transtensive and transpressive areas, or where they deform previous topographic features (e.g. Keller and Pinter, 2001). Forests extending across active fault zones can record the interplay between tectonic uplift and hillslope erosion (Jacoby, 1997; McCalpin, 2009). For example, tree trunks contain useful records of historic and prehistoric earthquakes along the San Andreas Fault in southern California (Jacoby *et al*., 1988), the Denali Fault in Alaska (Carver *et al*., 2004) and the North Anatolian Fault in Turkey (Kozaci, 2012).

The Magallanes–Fagnano fault system (MFFS) forms the active transform plate boundary between the South American and Scotia plates (e.g. Barker, 2001; Lodolo *et al*., 2003). The last major earthquake to shake Tierra del Fuego (Ms 7.8 on 17 December 1949) probably nucleated on this fault, and undated fault scarps on the MFFS may be associated with this event (Costa *et al*., 2006). A previous seismic event shook the region on 1 February 1879 (Modified Mercalli Scale, MMS VI), although the source of this earthquake is unknown. The aim of this study is to detect major rejuvenation of the Magallanes–Fagnano fault scarp by analysing annual tree-ring patterns in Lenga trees (*Nothofagus pumilio*) and testing whether they correlate with the last major historical and instrumental earthquakes.

Correspondence: Dr. Antonio Pedrera, Instituto Andaluz Ciencias de la Tierra, CSIC/Universidad de Granada, 18002 Granada, Spain. Tel.: +34 95 823 00 00; e-mail: pedrera@ugr.es

The Magallanes–Fagnano fault system

The MFFS extends ~650 km from the western limit of the Magallanes Strait to the Atlantic coast, cutting across Tierra del Fuego Island. The offshore trace of the MFFS continues ~2200 km across the North Scotia Ridge, up to the northern border of the East Scotia Ridge, close to the South Sandwich Islands (Fig. 1A). The plate boundary has a general E–W trend, which changes to WNW–ESE in the Magallanes section, with left-lateral kinematics (e.g. Klepeis, 1994; Lodolo *et al*., 2003). The MFFS has been active since the Tortonian (~11–7 Ma, Torres-Carbonell *et al*., 2008). Global Positioning System (GPS) measurements reveal that crustal deformation is clearly concentrated along the MFFS, mainly in the continental sector around Fagnano Lake, suggesting a present-day (period 1993–2008) horizontal slip rate of the fault zone of around 4.4 ± 0.6 mm a^{-1} (Mendoza *et al*., 2011). We focus our description on the eastern onshore section of the MFFS, from Fagnano Lake to the Atlantic coast (Figs 1B and C), where aerial and satellite imagery allows fault scarps to be mapped. There, the MFFS consists of several discontinuous fault segments, each from 5 to 15 km long, that develop parallel ridges and valleys (Figs 1 and 2) (Lodolo *et al*., 2003). A left-stepping extensional en echelon zone

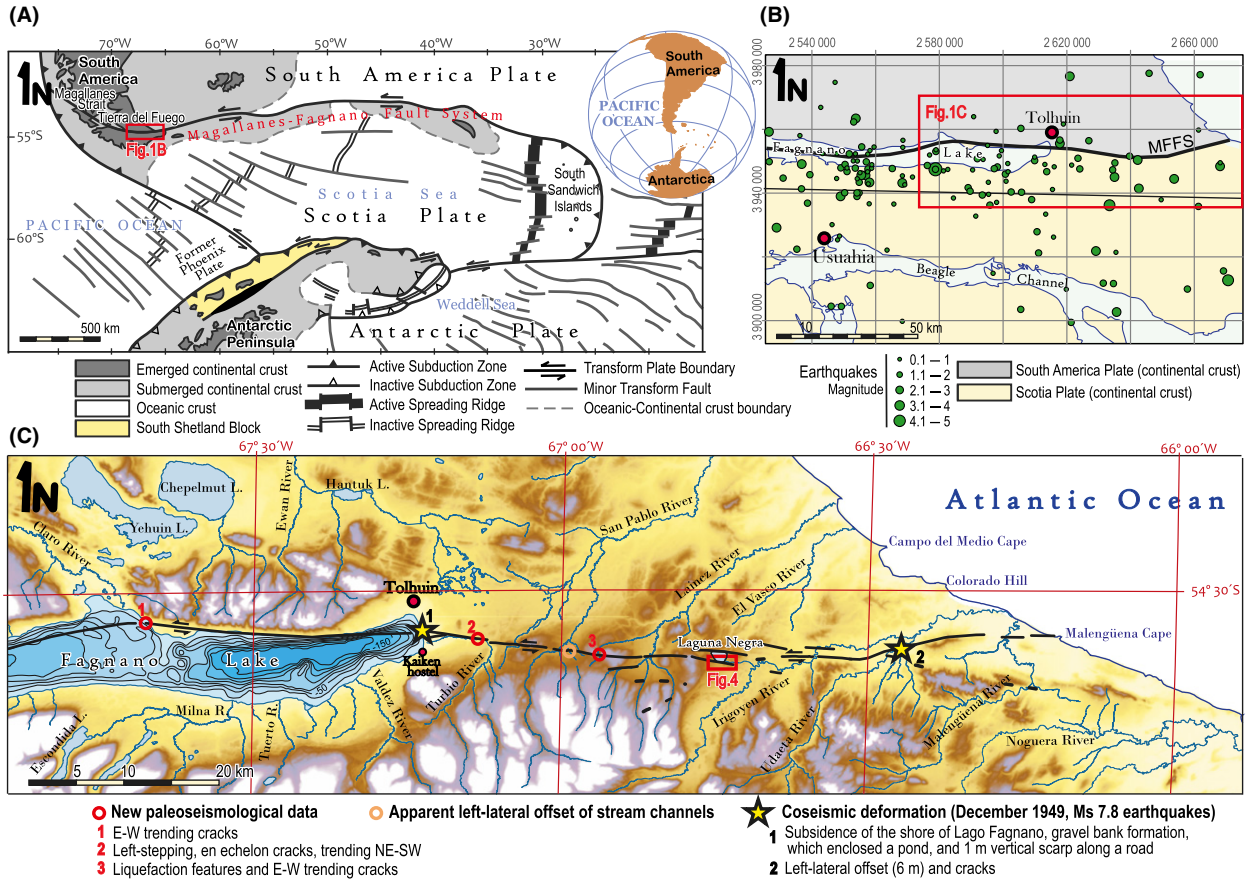

Fig. 1 (A) Tectonic setting of the Magallanes–Fagnano Fault System (MFFS) in the framework of the Scotia Arc. (B) Seismicity in the onshore eastern section of the MFFS after Sabbione *et al.* (2007a,b, 2011). (C) MFFS trace, main rivers and lakes plotted over the digital elevation model of Tierra del Fuego National Aeronautics and Space Administration (NASA) Shuttle Radar Topography Mission data (SRTM; Farr *et al.*, 2007). Bathymetric map of Fagnano Lake taken from Waldmann *et al.* (2011). The on-fault coseismic effects of the 1949 Ms 7.8 earthquake (Costa *et al.*, 2006), new palaeoseismological evidence and stream channels showing apparent left-lateral offset are also indicated. The location of the map in Fig. 4 is marked.

forms a small closed depression, the Laguna Negra bog (Figs 1C and 2B) (Menichetti *et al.*, 2001).

Seismicity in Tierra del Fuego is characterized by relatively frequent moderate earthquakes ($M \leq 5.0$) and rare large events ($M \geq 7$). Large earthquakes are mostly concentrated in the Scotia Plate above 30 km depth and located close to the MFFS (Fig. 1B) (Sabbione *et al.*, 2007a,b, 2011). The earliest large earthquake reported in Tierra del Fuego occurred on 1 February 1879 and was felt in Ushuaia with a MMS intensity of VI (Febrer *et al.*, 2000). The epicentre of this earthquake is unknown, but was tentatively placed offshore in the Atlantic Ocean (Febrer *et al.*, 2000). On 17 December 1949, a Ms 7.8 earthquake (MMS Intensity VIII) was strongly felt in the eastern Tierra del Fuego, near Fagnano Lake (Febrer *et al.*, 2000). Several coseismic features were recognized along the eastern onshore section of the MFFS (Winslow, 1982; Dalziel, 1989). A vertical scarp (~0.5–1 m) occurred in a gravel bar bordering the eastern side of Fagnano Lake (Fig. 1C). Coseismic subsidence along this shore of the lake formed a series of connected lagoons, damaging many trees (Figs 1C and 2D) (Menichetti *et al.*, 2001). Shear fractures with ~6 m lateral offset and open cracks were described close to the Irigoyen River near the Atlantic coast (Costa *et al.*, 2006). In addition, coseismic off-fault features such as cracks and liquefaction processes were reported further to the north. Coseismic deposits associated with two, or possibly three, palaeoearthquakes during the last 9 ka, previous to the 1949 earthquake, have been recognized and dated in trenches across the eastern MFFS (Costa *et al.*, 2006).

Methods

Nothofagus pumilio is a deciduous broad-leafed tree with a generally straight trunk that covers large areas in Tierra del Fuego. Some studies have used changes in tree-ring width and density to determine climate variations (Villalba *et al.*, 2003), and the record of scars in the wood to establish the snow avalanche occurrence (Mundo *et al.*, 2007). The sudden formation/rejuvenation of a fault scarp during an earthquake may tilt trees, stimulating disturbances in the growth-ring series (Jacoby *et al.*, 1988). Tilted trees naturally have the ability to recover verticality by developing J-shaped morphologies along the trunk (Scurfield, 1973; Fig. 3).

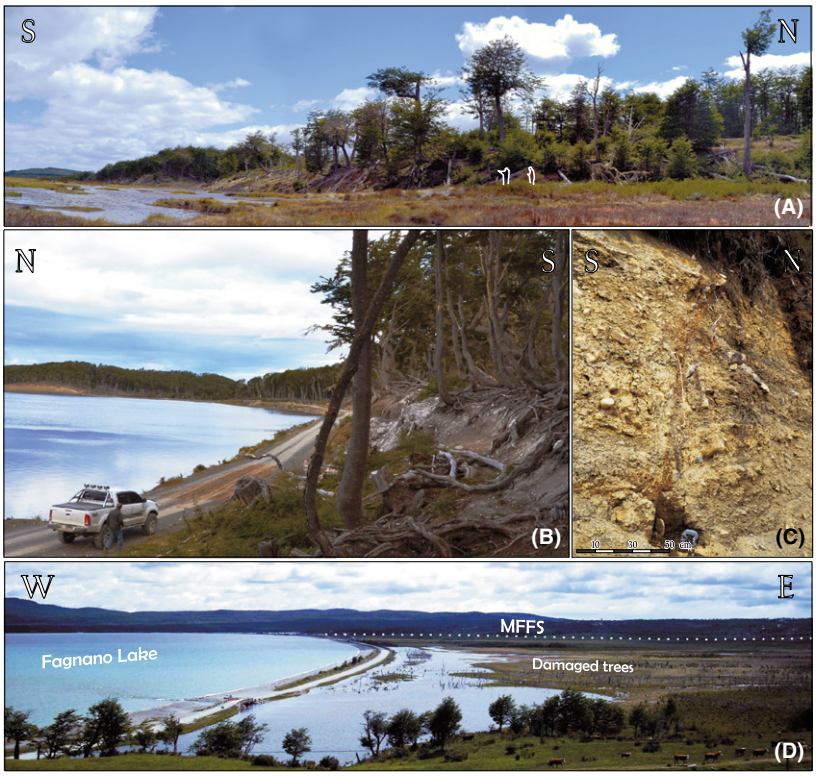

Fig. 2 Field photographs of the Magallanes–Fagnano Fault System. (A) Fault scarp at the San Pablo River sector. (B) Extensional fault scarp at the Laguna Negra bog. Note the bent lengas located on the fault scarp. (C) E–W trending crack where the fault system crosses the Lainez River (site 3 in Fig. 1). (D) Sector affected by coseismic subsidence that damaged trees along the eastern side of Fagnano Lake during the 1949 Ms 7.8 earthquake.

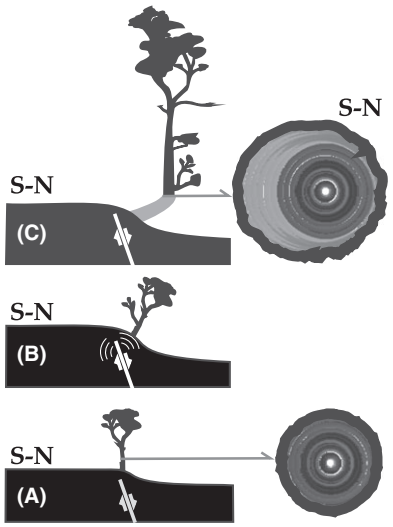

Fig. 3 Schematic sequence of lenga tree growth conditioned by the sudden formation of a coseismic fault scarp: (A) vertical trees with symmetric tree-ring growth; (B) scarp rejuvenation associated with a strong seismic event that tilted the trees and activated creep due to slope increase; (C) tree trunks recovering verticality and tree-ring asymmetry marking scarp development.

This process is recorded by the onset of asymmetric tree-ring growth (Timell, 1986), i.e. narrow annual rings on the tilted side and wide rings on the opposite side.

We examined complete cross-sections from 34 trees that were cut by the timber industry in 2007 (Fig. 4). Samples cover two complete transects across the southern fault segment in the Laguna Negra stepover, from the uplifted to the downthrown block. The trees were sanded in the field, and tree-rings were counted and ring widths measured directly in the field and in the laboratory using scaled and restored photographs. Uncertainties in the attribution of an age to some trees and rings resulted from unclear ring boundaries and the presence of spoiled areas. Four trees in a flat area close to the fault scarp and unaffected by tilting were also analysed. They show common ring width variations that enabled us to establish an accurate reference chronology, which is compared with the disturbed growth-ring patterns of the trees situated above the fault scarp. Determination of past earthquake events is based on the number of trees showing asymmetric growth onset in a specific year. To avoid overestimation, we used the index value (*It*) defined by Schroeder (1978) as the percentage of trees showing a reaction in a specific year compared with the sample trees alive in that year. The age of the analysed trees was between 62 and 180 years, providing a record back to 1827, balanced to include older and younger trees.

Results

Fault traces of the MFFS were recognized from Fagnano Lake to the Atlantic coast according to satellite imagery and field work. We identified fault scarps, stream channels showing an apparent left-lateral offset, and palaeoseismological evidence such as liquefaction features, E–W-trending cracks and NE–SW left-stepping en echelon cracks (Figs 1 and 2). Analysis of 34 trees in the Laguna Negra stepover, where the fault scarp is ~8 m high, allowed us to identify asymmetric ring growth related to past earthquakes (Figs 3C and 4A). Two clear disturbance events were detected where the onset of asymmetric growth-ring patterns interrupted the reference chronology. Seven tree trunks record asymmetric growth onset in 1941 ± 10 years (*It* = 23%) and eight in 1883 ± 5 years (*It* = 100%). In addition, 15 trees show an entirely asymmetric ring pattern, interpreted as growth on an already unstable slope. A group of 9 tree trunks has ages clustered around 1941 ± 10 years, and a group of just four older trees began growth in 1910 ± 5 years (Fig. 5 and Table S1).

Discussion

The perturbation in annual tree-ring growth patterns caused by seismic damage provides important information about the frequency and location

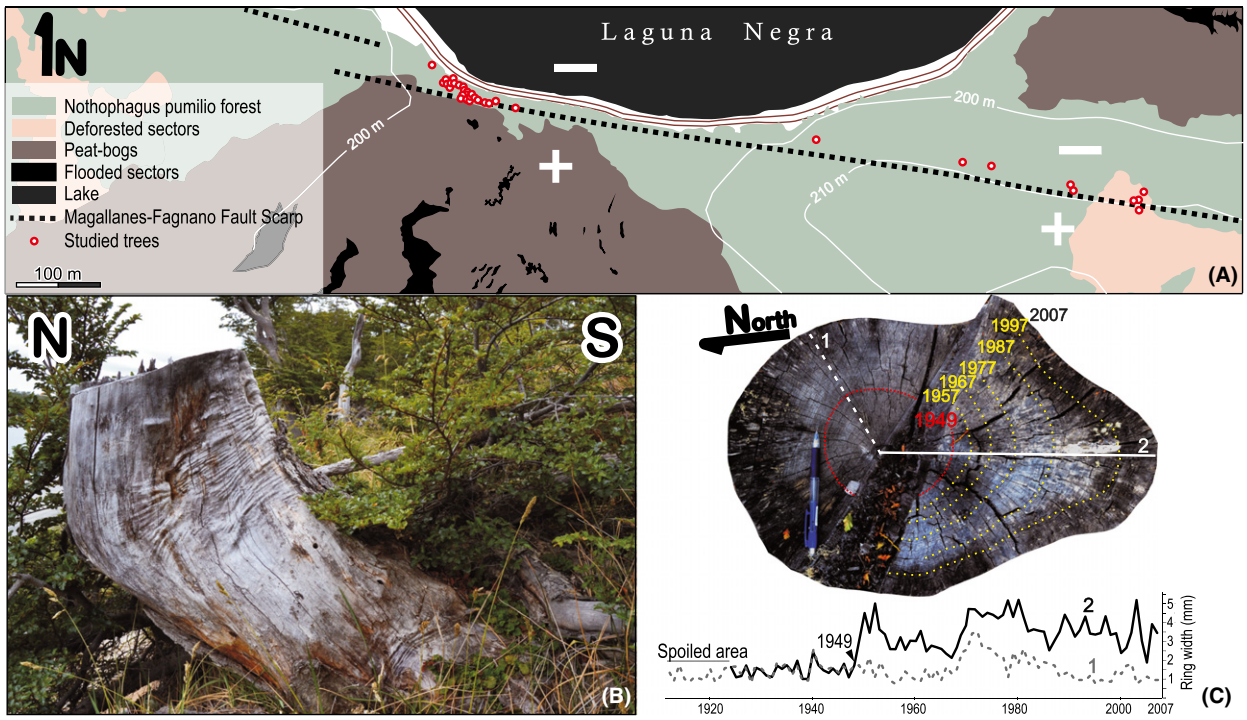

Fig. 4 (A) Map showing the southern fault segment (the main one) in the left-stepping extensional en echelon zone leading to the Laguna Negra bog, and the location of the studied trees. (B) Example of a curved tree trunk situated above the fault scarp (tree sample 1 in Fig. 5). (C) Growth ring pattern with symmetric–asymmetric transition in 1949.

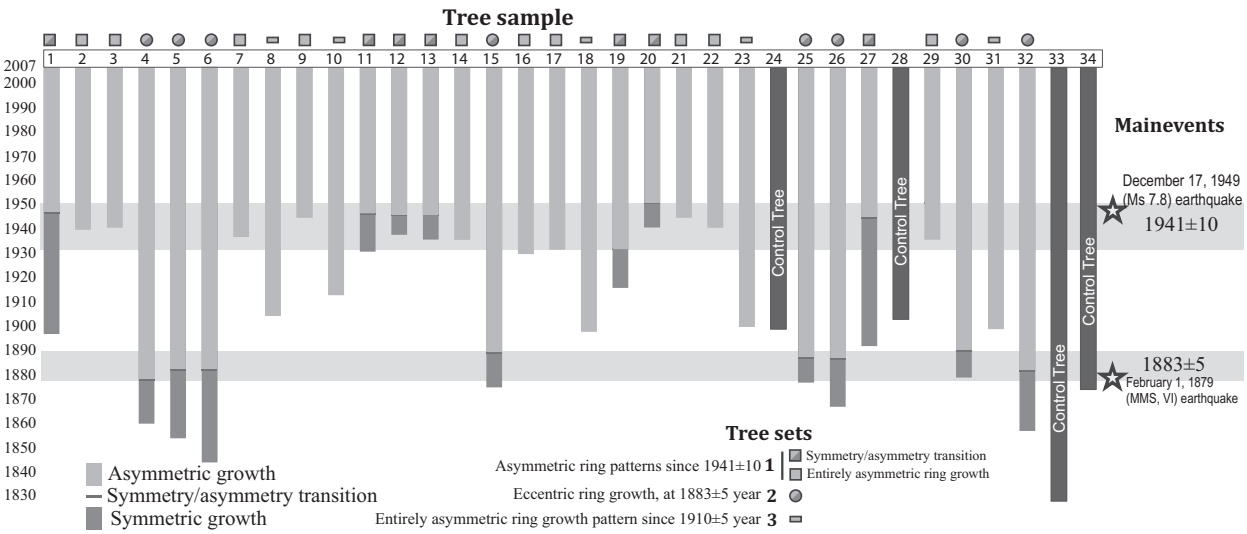

Fig. 5 The symmetric–asymmetric transitions of the studied lenga trees above the fault trace. The symmetric–asymmetric transition events coincide with the 1 February 1879 (Modified Mercalli Scale, VI) and the 17 December 1949 (Ms 7.8) major earthquakes.

of the seismic events. Trees may record palaeoearthquakes directly when they grow above the fault trace and are either tilted by the fault scarp formation or sheared by the fault plane. In addition, trees farther from the seismic fault could be damaged by coseismic subsidence and strongly influenced by shaking or other secondary effects such as landslides (Jacoby, 1997; McCalpin, 2009).

Ruptures associated with the 1949, Ms 7.8 earthquake extend at least ~50 km, from the eastern shore of Fagnano Lake to the Irigoyen River, revealing that the earthquake nucleated on the eastern onshore sector of

the fault. Evidence from the Atlantic coast at Malengüena Cape (Torres-Carbonell *et al.*, 2011) suggests that the ruptures could extend further eastwards. This would be in agreement with the empirical relationships between magnitude and rupture length, given that earthquakes with magnitudes between 7 and 8 usually have associated surface fault ruptures ranging from 50 to 300 km (Wells and Coppersmith, 1994). We found that this earthquake rejuvenated the fault scarp in the Laguna Negra releasing stepover, with a considerable dip-slip component, tilting the trees. Vertical motion (0.5–1 m) was described by inhabitants near Fagnano Lake, another releasing bend sector, where many trees were flooded due to coseismic subsidence during this seismic event (Costa *et al.*, 2006). On the other hand, the oldest studied trees record a change from symmetric to asymmetric growth in 1883 ± 5 years, coinciding with the 1 February 1879 earthquake (MMS VI), probably as a result of scarp rejuvenation during this earthquake.

Regarding the location of trees within the fault scarp, the trunks that show symmetry–asymmetry changes (7 trees in 1949 and 8 trees in 1879) started growing in a stable part of the scarp, although placed on the fault scarp. Scarp rejuvenation events during earthquakes trigger creep in these sectors by increasing the slope during the years following the earthquake. Some of the trees reach a new balance by bending upwards, but most of them present asymmetric growth until the end. The age uncertainties of ± 5 and ± 10 years are caused by the presence of false annual rings (triggered by an abrupt change in climate within one season), by the occurrence of missing rings (lack of growth following damage), and also by a delayed response of specific trees to the surface deformation. In our example, part of the fault scarp remains unstable giving rise to trees showing an entirely asymmetric ring pattern. Three main reasons could explain why some trees would not be tilted by a given seismic event: the location of the tree within the fault scarp, the degree of tilting, and the age/size of the tree when the event occurs. Regarding the size of the tree, if the tilted tree is older than ~50 years, it lacks the ability to recover verticality (Fig. 5). This is probably due to its size, as smaller trees can easily reorientate after tilting.

To discard the possibility that the slope processes detected in our study could be driven by climatic causes, we examined climatic controlled slope processes occurring in other parts of Tierra del Fuego. Mundo *et al.* (2007) examined geomorphic events affecting the *Nothofagus pumilio* forest on the western hillside of Martial Valley (Tierra del Fuego). The slope of the valley (30–45°) is equivalent to the slope of the fault scarp studied here. Their study confirmed a climatic-controlled avalanche in 1976, based on scars, changes in radial growth patterns and climate data. This regional climatic event was not recorded by the trees on the fault scarp, and the Martial Valley trees on similar slopes, but away from the fault, does not show the earthquake signatures.

Elastic rebound theory predicts that the major earthquakes on a fault are time dependent, as they are linked to a period of built-up energy (interseismic) with abrupt relaxation stages (coseismic). Both the short-term geodetic (Mendoza *et al.*, 2011) and the long-term geological slip rates of the MFFS are low (~5 mm a^{-1}) (Torres-Carbonell *et al.*, 2008). Therefore, the time span between major earthquakes should be larger than the one obtained. Considering a simple tectonic setting of a pure left-lateral strike-slip fault with a constant 5 mm a^{-1} slip rate (geodetic slip rate, Mendoza *et al.*, 2011) able to generate ~6 m of left-lateral maximum displacement at the surface during the largest earthquakes (effects of the 1949 Ms 7.8 earthquake; Costa *et al.*, 2006), the expected time span between comparable earthquakes would be around 10 ka. Yet the time between the two most recent large earthquakes on the eastern onshore fault section of the MFFS was about 70 years. Such a great discrepancy could result from the presence of locked sections and/or variable slip rate history, the lack of accurately documented surface ruptures for the calculations, and/or the complexities of the extensional en echelon geometry of the MFFS in the study area. Further work is needed to assess this question. Notwithstanding, our results fill the time gap between the 1949 event and the two, possibly three, palaeoearthquakes detected by trenching during the last 9 ka (Costa *et al.*, 2006) and suggest a complex earthquake type ($M \geq 7$) recurrence on the MFF.

Conclusions

Tree-ring analysis suggests rupture on the MFFS fault scarp in 1883 ± 5 and 1941 ± 10, coinciding with the 1 February 1879 (Modified Mercalli Scale, VI) and 17 December 1949 (Ms 7.8) earthquakes in Tierra del Fuego. Our contribution encourages the study of disturbed trees growing over seismic faults. This line of research is very useful in areas like Tierra del Fuego with an incomplete catalogue of historical earthquakes and a very short instrumental seismicity record.

Acknowledgements

This study was supported by project CTM2011-30241-C02-02 and the group RNM-148. We thank M. Pérez and M. Barbagallo (CADIC-CONICET) for transportation, CADIC for accommodation, and R. Garibaldi for granting access to the field. We really acknowledge the positive reviews of Lucilla Benedetti and Ozgur Kozaci. Jean Louise Sanders revised the English style.

References

Barker, P.F., 2001. Scotia Sea regional tectonic evolution: implications for mantle flow and paleocirculation. *Earth Sci. Rev.*, **55**, 1–39.

Carver, G., Plafker, G., Metz, M., Cluff, L., Slemmons, B., Johnson, E., Roddick, J. and Sorensen, S., 2004. Surface rupture on the Denali Fault interpreted from tree damage during the 1912 Delta river M w 7.2-7.4 earthquake: implications for the 2002 Denali Fault earthquake slip distribution. *Bull. Seismol. Soc. Am.*, **94**, S58–S71.

Costa, C.H., Smalley, J.R., Schwartz, D.P., Stenner, H.D., Ellis, M., Ahumada, E.A. and Velasco, M.A., 2006. Paleoseismic observations of an onshore transform boundary: the Magallanes-Fagnano fault, Tierra Del Fuego, Argentina. *Rev. Asoc. Geol. Argent.*, **61**, 647–657.

Dalziel, I.W.D., 1989. Tectonics of the Scotia Arc, Antarctica. Field Trip Guide, T180, 206 p.

Farr, T.G., Rosen, P.A., Caro, E., Crippen, R., Duren, R. and Hensley, S., 2007. The Shuttle radar topography mission. *Rev. Geophys*., **45**, RG2004.

Febrer, J.M., Plasencia, M.P. and Sabbione, N.C., 2000. Local and regional seismicity from Ushuaia broadband station observations (Tierra del Fuego). *Terra Antarct*., **8**, 35–40.

Jacoby, G.C., 1997. Application of tree-ring analysis to paleoseismology. *Rev. Geophys*., **35**, 109–124.

Jacoby, G.C., Sheppard, P.R. and Sieh, K.E., 1988. Irregular recurrence of large earthquakes along the San Andreas fault: evidence from trees. *Science*, **241**, 196–199.

Keller, E.A. and Pinter, N., 2001. *Active Tectonics: Earthquakes, Uplift, and Landscape*, 2nd edn. Prentice Hall, Upper Saddle River, NJ, 362 p.

Klepeis, K.A., 1994. The Magallanes and Deseado fault zones: major segments of the South American-Scotia transform plate boundary in southernmost South America, Tierra del Fuego. *J. Geophys. Res*., **99**, 22001–22014.

Kozaci, Ö., 2012. Dendroseismology on the central North Anatolian fault, Turkey: documenting three centuries of surface rupture history using tree rings. *J. Geophys. Res*., **117**, B01405.

Lodolo, E., Menichetti, M., Bartole, R., Ben-Avraham, Z., Tassone, A. and Lippai, H., 2003. Magallanes-Fagnano continental transform fault (Tierra del Fuego, southernmost South America). *Tectonics*, **22**, 1076.

McCalpin, J.P., 2009. *Paleoseismology*, 2nd edn., International Geophysics Series. Elsevier, Amsterdam. 613 p.

Mendoza, L., Perdomo, R., Hormaechea, J.L., Cogliano, D.D., Fritsche, M., Richter, A. and Dietrich, R., 2011. Present-day crustal deformation along the Magallanes-Fagnano fault system in Tierra del Fuego from repeated GPS observations. *Geophys. J. Int*., **184**, 1009–1022.

Menichetti, M., Lodolo, E., Tassone, A. and Geletti, R., 2001.Neotectonics at the Continental Transform Boundary of the South America-Scotia Plates: The Magallanes-Fagnano Fault System. Terra Antartica Publication, Antarctic Neotectonic workshop, Siena, p. 55.

Mundo, I.A., Barrera, M.D. and Roiga, F.A., 2007. Testing the utility of Nothofagus pumilio for dating a snow avalanche in Tierra del Fuego, Argentina. *Dendrochronologia*, **25**, 19–28.

Sabbione, N., Connon, G., Hormaechea, J.L. and Rosa, M., 2007a. Estudio de sismicidad en la Provincia de Tierra del Fuego, Argentina. *Geoacta*, **32**, 41–50.

Sabbione, N., Connon, G., Buffoni, C. and Hormaechea, J.L., 2007b. Tierra del Fuego reference standard earthquake catalogue. Geosur 2007 International Geological.

Sabbione, N.C., Connon, G.C., Hormaechea, J.L. and Buffoni, C., 2011. Complemento al Catálogo Sismológico de Referencia para Tierra del Fuego. Estación Astronómica Río Grande. Unpublished Report.

Schroeder, J.F., Jr, 1978. Dendrogeomorphological analysis of mass movement on Table Cliffs Plateau. *Utah. Quat. Res*., **9**, 168–185.

Scurfield, G., 1973. Reaction wood: its structure and function lignification may generate the force active in restoring the trunks of leaning trees to the vertical. *Science*, **179**, 647–655.

Timell, T.E., 1986. *Compression Wood in Gymnosperms*. Springer, Berlin.

Torres-Carbonell, P.J., Olivero, E.B. and Dimieri, L.V., 2008. Constraints on the magnitude of strike-slip displacement along the Fagnano Transform System, Tierra del Fuego, Argentina. *Rev. Geol. Chile*, **35**, 63–77.

Torres-Carbonell, P.J., Dimieri, L.V. and Olivero, E.B., 2011. Progressive deformation of a Coulomb thrust wedge: the eastern Fuegian Andes Thrust-Fold Belt. In: *Kinematic Evolution and Structural Styles of Fold-and-Thrust Belts* (J. Poblet and R. Lisle, eds.). *Geol. Soc. London Spec. Publ*., **349**, 123–147.

Villalba, R., Lara, A., Boninsegna, J.A., Masiokas, M., Delgado, S., Aravena, J.C., Roig, F.A., Schmelter, A., Wolodarsky, A. and Ripalta, A., 2003. Large-scale temperature changes across the Southern Andes: 20th-century variations in the context of the past 400 years. *Climatic Change*, **59**, 177–232.

Waldmann, N., Anselmetti, F.S., Arizteguin, D., Austin, J.A., Jr., Pirouzn, M., Moyz, C.M. and Dunbark, R., 2011. Holocene mass-wasting events in Lago Fagnano, Tierra del Fuego (54°S): implications for paleoseismicity of the Magallanes-Fagnano transform fault. *Basin Res*., **23**, 171–190.

Wells, D.L. and Coppersmith, K.J., 1994. New empirical relationships among magnitude, rupture length, rupture width, rupture area and surface displacement. *Bull. Seismol. Soc. Am*., **84**, 974–1002.

Winslow, M.A., 1982. The structural evolution of the Magallanes Basin and neotectonics in the southernmost Andes. In: *Antarctic Geoscience* (C. Craddock, ed.), pp. 143–154. University of Wisconsin Press, Madison.

Yeats, R.S. and Prentice, C.S., 1996. Introduction to special section: paleoseismology. *J. Geophys. Res*., **101**, 5847–5853.

Received 14 February 2014; revised version accepted 22 July 2014

Supporting Information

Additional Supporting Information may be found in the online version of this article:

Table S1. Data repository.

